Food Chemistry 220 (2017) 25–30

Contents lists available at ScienceDirect

Food Chemistry

journal homepage: www.elsevier.com/locate/foodchem

Insights into molecular structure and digestion rate of oat starch

Jinchuan Xu [a,b], Qirong Kuang [b], Kai Wang [c], Sumei Zhou [b], Shuo Wang [a], Xingxun Liu [b,*], Shujun Wang [a,*]

[a] Key Laboratory of Food Nutrition and Safety, Ministry of Education, Tianjin University of Science & Technology, Tianjin 300457, China
[b] Institute of Food Science and Technology (IFST), Chinese Academy of Agricultural Science (CAAS), Beijing 100193, China
[c] College of Food Science, South China Agricultural University, Guangzhou 510640, China

ARTICLE INFO

Article history:
Received 15 July 2016
Received in revised form 22 September 2016
Accepted 28 September 2016
Available online 29 September 2016

Keywords:
Oat starch
Starch digestibility
Amylose
Amylopectin
Fine structure

ABSTRACT

The *in vitro* digestibility of oat starch and its relationship with starch molecular structure was investigated. The *in vitro* digestion results showed that the first-order kinetic constant (k) of oat starches (OS-1 and OS-2) was lower than that of rice starch. The size of amylose chains, amylose content and degree of branching (DB) of amylopectin in oat starch were significantly higher than the corresponding parameters in rice starch. The larger molecular size of oat starch may account for its lower digestion rate. The fine structure of amylopectin showed that oat starch had less chains of DP 6–12 and DP > 36, which may explain the small difference in digestion rate between oat and rice starch. The biosynthesis model from oat amylopectin fine structure data suggested a lower starch branching enzyme (SBE) activity and/or a higher starch synthase (SS) activity, which may decrease the DB of oat starch and increase its digestion rate.

1. Introduction

Oat is an important grain crop for humans, and is mainly grown in Russia, Canada, United States, Finland, Australia, and China (Xu, Ren, Liu, Zhu, & Liu, 2014). *Avena sativa* L. (hulled oat) and *Avena nuda* L. (naked oat) are two important cultivated oat species (Pu & Hu, 2012). Naked oat is commonly grown and consumed in north China, such as Shanxi, Gansu, Jilin and Hebei provinces. It is also used as a traditional Chinese medicine for hundreds of years (Hu, Zheng, Li, Xu, & Zhao, 2014). In contrast, hulled oat is widely grown in western countries and consumed in the form of rolled oats and steel-cut groats. Oat is recognized as a low or medium Glycemic Index (GI) food, depending on the processing protocols or cooking practices (Tosh & Chu, 2015). Starch is the major glycemic carbohydrate component in oat grains and accounts for above 60% of the dry matter (Zhou, Robards, & Glennie, 1998). The size of individual oat starch granule varies from 3 to 10 μm (Wang and White, 1994), much smaller than that of wheat, rye, barely and corn starch granules. The amylose content of oat starches is in the range of 25.2–29.4% (Gudmundsson & Eliasson, 1989).

As a major glycemic carbohydrate in the human diet, starch contributes over 50% of the total caloric intake in western countries and 90% in developing countries. A higher starch digestion rate may increase the risk of obesity, type II diabetes and cardiovascular disease (Wang, Li, Copeland, Niu, & Wang, 2015). Starch is composed of two types of glucans: amylose, an essentially linear structure of α-1,4-linked glucan, and amylopectin, a highly branched macromolecule with an average 5% of α-1,6-linkages. The relative portions of amylose and amylopectin in starch granules and their chain length distributions have profound influence on the digestion properties of starch (Hoover, Vasanthan, Senanayake, & Martin, 1994; Syahariza, Sar, Hasjim, Tizzotti, & Gilbert, 2013). Chung, Liu, Lee, and Wei (2011) found that raw rice starches with high amylose content have larger amounts of slowly digestible starch (SDS) and resistant starch (RS). Syahariza et al. (2013) showed that amylose content, degree of branching and fine molecular structural features all influence the digestion rate of cooked rice starches.

As a low to medium GI food, oat meal is a good option for those who are concerned about blood glucose responses to foods. Oats are almost always consumed as whole grains, in which non-starch components such as β-glucan, has been shown to decrease the susceptibility of starch to enzymatic digestibility (Pu & Hu, 2012). However, there is little information regarding the digestibility of oat starch and its relationship with molecular structure of oat starch. Hence, the objective of this study was to gain a better understanding of the relationship between molecular structure and digestibility of cooked oat starch. Since starch ordered structures are greatly disrupted during cooking (Syahariza et al., 2013; Wang & Copeland, 2013), only starch molecular structures will be considered. In this study, four representative oat varieties

* Corresponding authors.
E-mail addresses: ytboy652@163.com (X. Liu), sjwang@tust.edu.cn (S. Wang).

http://dx.doi.org/10.1016/j.foodchem.2016.09.191
0308-8146/

grown in typical locations in China were chosen, and one common rice variety (a high GI food) was used for reference. The molecular size distributions and chain-length distributions (CLDs) of debranched starches were analyzed using gel-permeation chromatography (GPC) and high-performance anion-exchange chromatography (HPAEC), respectively. Amylopectin CLDs were fitted using a mathematical model developed by Wu, Morell, and Gilbert (2013) to understand the activity of enzymes involved in starch biosynthesis. The resulting information will be beneficial for breeding new oat varieties with desired digestion properties.

2. Materials and methods

2.1. Materials

Four polished oat grains and one polished rice grain were collected from typical locations in China. The origins and suppliers of these grains are summarized in Table 1. The reference rice (an identified high GI variety) was used for comparison. Isoamylase (Megazyme, 1000 U/mL), pullulanase M1 (Megazyme, 700 U/mL), pepsin (Sigma P-6887, from gastric porcine mucosa), a-amylase (Sigma A-3176, 250 U/mL, from porcine pancreas), pancreatin (porcine pancreas at 4 × USP activity, Sigma P-1750) and amyloglucosidase (Megazyme E-AMGDF, 3300 U/mL) were used.

2.2. Starch extraction

Starch was extracted from oat and rice grains according to Wang, Zhang, Wang, and Copeland (2016) with minor modifications as follows. Briefly, polished oat and rice grains (300 g, respectively) were steeped in 900 mL of 0.45% (w/v) sodium pyrosulfite solution and stirred mechanically at 25 °C overnight. The supernatant was decanted, and swollen grains were mixed with 900 mL of 0.45% (w/v) sodium pyrosulfite solution and blended in a kitchen blender for 5 min at a low speed. The homogenate was then passed through a stainless steel sieve (150 μm) and centrifuged at 2000*g* for 15 min. The supernatant was discarded, and the sediment was suspended in excess water and centrifuged at 2000 g for 15 min. The procedure was repeated five times. The final sediment was suspended in absolute ethanol, passed through a 100 μm polypropylene sieve, and thoroughly washed with distilled water on a Buchner funnel. The filter cake was freeze-dried and ground using a mortar and pestle.

2.3. Gel-permeation chromatography (GPC)

Native starch granules (6 mg) were dissolved in DMSO/LiBr solution and debranched using isoamylase in acetate buffer (pH ~ 3.5), following the method of Li, Hasjim, Dhital, Godwin, and Gilbert (2011). The weight distributions of debranched starch molecules were analyzed in duplicate using GPC (Agilent 1260 series, Agilent Technologies, USA) equipped with a refractive index detector (Optilab T-rEX, WYATT Corp., USA), and a differential pressure detector (Viscostar-II, WYATT Corp., USA). GPC separates molecules based on their hydrodynamic volume (V_h), or the corresponding hydrodynamic radius (R_h). The GPC weight distributions, W ($\log V_h$), of debranched starch is denoted by W_{de} ($\log V_h$); the degree of polymerization (DP) of debranched starch, amylose content and degree of branching (DB) were calculated following the method described elsewhere (Wang et al., 2015).

2.4. High-performance anion-exchange chromatography (HPAEC)

Amylopectin fractionation was carried out according to the method of Kong, Bertoft, Bao, and Corke (2008). The fractionated amylopectin (3 mg) was dissolved in 150 mL 100% DMSO with constant stirring overnight. The solution was diluted with 750 mL MilliQ water, and 100 mL 0.1 M sodium acetate buffer (pH 5.5), 1 μL isoamylase and 1 μL pullulanase were added. The debranching reaction was conducted at room temperature with constant stirring overnight and terminated by heating at 100 °C. The sample was centrifuged at 10,000*g* for 15 min at 4 °C and filtrated (pore size 0.45 μm) before being injected to the HPAEC system.

The chain length distribution of debranched samples was analyzed following a method modified from a previous report (Kong et al., 2008) using a HPAEC system (DIONEX ICS-3000 USA) coupled with a BioLC gradient pump and a pulsed amperometric detector (PAD). PAD signal was recorded by PowerChrom software and corrected to carbohydrate content. Prior to loading the sample, the columns (Carbo-Pac PA-200 with a guard column) were flushed with 100 mM NaOH at a rate of 0.4 mL/min for 20 min, followed by a mixture of two eluents: 100 mM NaOH (eluent A, 96%) and 100 mM NaOH containing 500 mM NaOAc (eluent B, 4%) for another 20 min. The elution gradient at a rate of 0.4 mL/min was as follows: from 0 to 45 min, 96% eluent A; from 45 to 80 min, eluent A changed from 96 to 40% linearly; from 80 to 95 min, from 40 to 20%; from 95 to 105 min, from 20 to 96% (returned to start mixture).

2.5. In vitro digestibility of cooked starch

The *in vitro* digestion of starch was analyzed following a three-stage digestion protocol described elsewhere (Chen et al., 2016). Exactly 200 mg of starch in a flask was cooked with 1.0 ml of deionized water in a boiling water bath for 30 min with stirring at a speed of 300 rpm. After cooling to 37 °C, 1.0 mL artificial saliva solution containing 250 U pancreatic α-amylase was added. After 1 min incubation, 5 mL of 0.02 M HCl solution containing porcine pepsin (3200 U) was added and the mixture was incubated at 37 °C for 30 min with stirring at 100 rpm. The solution was neutralized with 5 mL of 0.02 M NaOH and mixed with 25 mL of 0.2 M sodium acetate buffer (pH = 6). Pancreatin (2 mg/mL, activity of 4 × U.S.P specification) and 140 U amyloglucosidase in the same sodium acetate buffer solution (5 mL) was added to the digesta, and the mixture was incubated at 37 °C with stirring at 100 rpm. At specified time points (0, 10, 20, 30, 40, 50, 60, 70, 80, 90, 120 and 180 min), 200 μL aliquots were withdrawn and mixed with 750 μL of 95% ethanol to stop enzymic reaction. The amount of glucose released was determined using the Megazyme GOPOD kit. The percentage of hydrolysed starch was calculated by multiplying the

Table 1
Sources of oat and rice starches and digestion parameters obtained from LOS plots of starch digestograms.

Variety	Code	Province	Moisture (%)	$k \times 10^{-2}$ (min^{-1})	C_∞ (%)
Baiyan4	OS-1	Gansu	7.95 ± 0.04c	2.81 ± 0.05c	83.63 ± 0.19a
Baiyan2	OS-2	Jilin	8.05 ± 0.08c	3.19 ± 0.10bc	83.67 ± 1.07a
Bayou1	OS-3	Hebei	7.97 ± 0.04c	3.48 ± 0.01ab	83.20 ± 0.27a
Huazao2	OS-4	Hebei	13.19 ± 0.03a	3.69 ± 0.00a	80.56 ± 0.94b
Xing2	RS	Hunan	12.06 ± 0.02b	3.66 ± 0.33a	84.68 ± 0.67a

Values are means ± standard deviation. Values with different letters in the same column are significantly different at $p < 0.05$.

glucose content with a factor of 0.9. The digestograms were fitted to the first-order kinetics (Butterworth, Warren, Grassby, Patel, & Ellis, 2012; Edwards, Warren, Milligan, Butterworth, & Ellis, 2014) as shown in Eq. (1):

$$C_t = C_\infty(1 - e^{-kt}) \quad (1)$$

where C_t is the concentration of product at a given time (t), C_∞ is the concentration of product at the end of the reaction, and k is the first order rate constant. For ease of interpretation, C_t may be expressed as the amount of starch digested as a percentage of the total starch content of sample.

A Logarithm of Slope (LOS) plot was obtained by expressing the first derivative of the first-order equation in logarithmic form (Eq. (2)).

$$\ln\left(\frac{dC}{dt}\right) = -kt + \ln(C_\infty k) \quad (2)$$

where $\ln(dC/dt)$ represents the logarithm of the slope, and the equation describes a linear relationship between LOS and time of amylolysis, t. The resulting k and C_∞ were used to construct model-fit starch digestion curves according to Eq. (1), and residual analysis was employed to compare experimental data to the starch digestion curves generated by the model fit.

2.6. Fitting the amylopectin number CLD with a mathematical model

The number CLD of amylopectin characterized using HPAEC was fitted with an amylopectin biosynthesis-based model to obtain information on the starch biosynthetic enzymes (Wu & Gilbert, 2010). The underlying theory of this model is that a number of enzyme sets, with each set comprising of a various isoforms of starch synthases (SSs), starch branching enzymes (SBE) and debranching enzymes (DBE) control the amylopectin CLDs. By fitting the number CLD of amylopectin with this model, parameters indicating activity ratio of SBE to SS (denoted by β), and the relative contribution of each enzyme set to the entire amylopectin CLD (denoted by h) can be obtained (Wu et al., 2013).

2.7. Statistical analysis

For each structural measurement, analyses were performed in duplicate for each sample. All data were reported as mean ± standard deviation (SD) using analysis of variance (ANOVA) with Tukey's pairwise comparison. Significant differences of the mean values were determined at $p < 0.05$. The starch digestibility measurements were analyzed at least duplicate for each sample. One-way analysis of variance (ANOVA) method was carried out using SPSS V. 22.0 software (SPSS Inc., Chicago, IL).

3. Results and discussion

3.1. In vitro digestibility of cooked starch

The logarithm of the slope (LOS) plot approach is used to study and interpret starch digestibility *in vitro*, and in turn to predict the physiological responses (Patel, Day, Butterworth, & Ellis, 2014; Poulsen, Ruiter, Visser, & Lønsmann Iversen, 2003; Wilfart, Simminsb, Nobleta, van Milgena, & Montagnec, 2008; Zou, Sissons, Gidley, Gilbert, & Warren, 2015). The LOS plot can be used to quantify the differences in digestion rate during starch amylolysis and predict the product concentration at the end of amylolysis without the need to carry out prolonged digestion (Edwards et al., 2014). This end product is the total amount of starch digested in the food and is referred to as *C* infinity (C_∞).

The typical digestograms and fit of the data to first-order kinetics equation for starch hydrolysis are shown in Figs. 1 and S1. The k and C_∞ values obtained from the LOS plot derived from the first-order kinetics for starch digestion are given in Table 1. Starch was digested rapidly during the initial one hour and nearly reached a plateau at 60–80 min (Fig. 1). All the LOS plots of starch showed the linear relationship with a constant k, indicating that the digestion of freshly cooked starch is a single-phase process. The k value of rice starch was significantly higher than that of oat starch-1 (OS-1) and oat starch-2 (OS-2), and comparable to oat starch-3 (OS-3) and oat starch-4 (OS-4) (Table 1). C_∞ represents the theoretical percentage of starch digested at the reaction end point. OS-4 showed a lower C_∞ value compared with other starches, suggesting that OS-4 was less digestible than other starches.

3.2. Molecular structure of starches

The GPC weight CLDs, $W_{de}(\log X)$, of individual chains obtained from debranched starch as a function of DP X are shown in Fig. 2. The components with X < 100 (about Rh 0.5–6 nm) are defined as amylopectin chains, while those with X > 100 (Rh > 6 nm) are defined as amylose chains (Vilaplana & Gilbert, 2010; Wang, Wambugu, et al., 2015). The typically bimodal distribution was

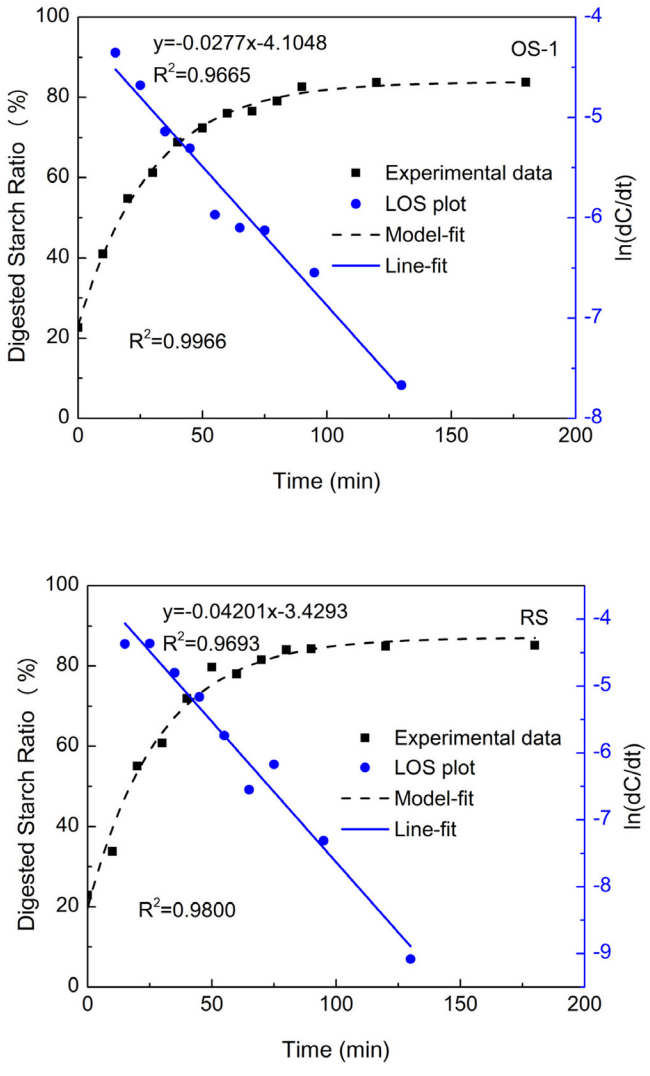

Fig. 1. Typical starch digestion curves, model-fit curves and LOS plots from oat and rice starch.

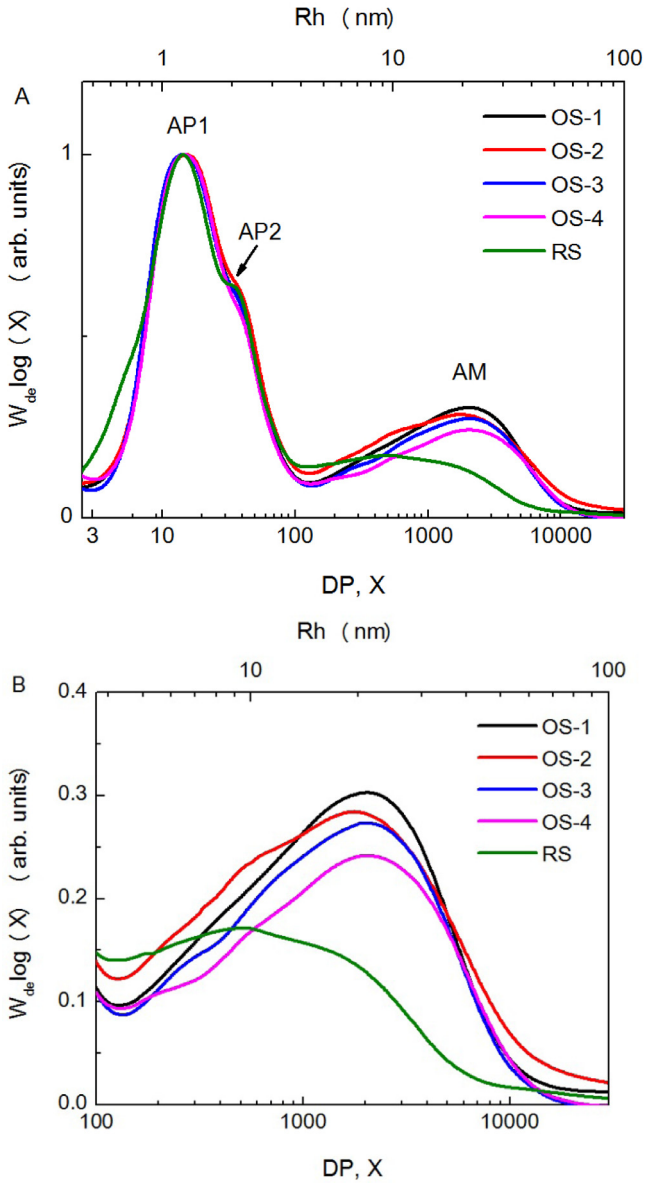

Fig. 2. GPC weight chain-length distributions, $W_{de}(\log X)$, of (A) debranched starches and (B) an enlargement of the amylose region as a function of DP *X*.

observed for amylopectin chains of all samples, while multiple small bumps were observed for amylose chains. The amylopectin chains could be further divided into AP1 and AP2 (Fig. 2A), corresponding to short and long chains of amylopectin, respectively. The first peak (denoted AP1) is the global maximum, which comprises the shorter amylopectin branches with lengths up to a DP of 37 (Rh 0.5–2 nm); these are confined to one amorphous/crystalline lamella. The second peak or shoulder (denoted AP2) are longer amylopectin branches with DPs ranging from 37 to 100 (Rh 2–4.5 nm), which span more than one crystalline lamella (Li, Prakash, Nicholson, Fitzgerald, & Gilbert, 2016). The amylose content was obtained from the weight CLD curves by calculating the ratio of the AUC of the whole amylose range (DP 100–30,000) to the AUC of the debranched starch distribution (DP-30,000) (Syahariza et al., 2013).

As observed in Fig. 2 and Table 2, the amylose content of oat starches was significantly higher than that of rice starch, although no significant differences were noted between oat starches. Themolecular size of amylose chains in oat starches was about 20–25 nm, much higher than that in rice starch (about 10 nm). On the other hand, oat starches also showed a lower proportion of short amylopectin chains with DP < 10 (Rh ~ 1 nm).

To compare the fine structure of various starches, a set of empirical parameters were obtained from GPC results (Syahariza et al., 2013). DPs at the maximum of each peak are donated X_{AP1}, X_{AP2}, X_{AM}, the height at each peak maximum are denoted H_{AP1}, H_{AP2} and H_{AM}, and the ratio of the peak height of AM to that of AP1 is denoted H_{AM}/H_{AP1}. The AUC_{AP1} and AUC_{AP2} are taken as the ratio of the area under the curve (AUC) of AP1 and AP2 branches to the AUC of the entire distribution curve (including both AP and AM branches). The parameters obtained from Fig. 2 are displayed in Table 2. The degree of branching of oat starches was lower than that of rice starch, indicating that rice starch contains a higher amount of branch points. OS-1, OS-2 and OS-3 presented the highest H_{AM}/H_{AP1} values, followed by OS-4, while rice starch showed the lowest value. The AUC_{AP1} and AUC_{AP2} values of rice starch were higher than those of oat starches, although the differences of AUC_{AP2} between oat and rice starches were not significant in some cases. Significant differences were observed in the X_{AM} values between rice and oat starches. The X_{AP1} values, however, were statistically similar between the samples.

3.3. Chain-length profiles of amylopectin from all starches

The typical weight-based and molar-based chain-length profiles of debranched amylopectin are shown in Fig. S2, and the parameters of chain length distribution and average chain length of amylopectin are summarized in Table 4. The first peak of weight-based bimodal chain-length profiles for all tested oat amylopectin was at DP ~ 13, and the second peak was at DP ~ 44 (Kong et al., 2008). A shoulder at DP 20–22 was observed for all amylopectin samples. Although the peak corresponding to the chains with DP > 66 were not observed clearly in HPAEC spectra (see Fig. S2), the amount of these chains was still calculated by integrating the corresponding chromatogram peak for each chain.

Amylopectin from the oat and rice starches showed similar chain length distribution profiles. The molar- and weight-based chain-length distributions of debranched amylopectin can be grouped into four fractions (Kong et al., 2008): A (DP ~ 6–12), B_1 (DP ~ 13–24), B_2 (DP ~ 25–36) and B_3 (DP ⩾ 37). There were significant differences in the proportion of each group of amylopectin chains between oat and rice starch samples (Table 3), but oat starches showed similar chain length distribution profiles. As seen

Table 2
Structural parameters of amylose and amylopectin from starch samples.

Code	AUC_{AP1}	AUC_{AP2}	X_{AP1}	X_{AM}	H_{AM}/H_{AP1}	AM (%)	DB (%)
OS-1	0.511 ± 0.005b	0.169 ± 0.012ab	14.674 ± 0.287ab	2115 ± 15a	0.293 ± 0.013a	32.03 ± 1.72a	4.99 ± 0.07 c
OS-2	0.509 ± 0.022b	0.170 ± 0.004ab	15.241 ± 0.222a	1771 ± 10b	0.289 ± 0.006a	32.09 ± 2.67a	5.03 ± 0.10 c
OS-3	0.523 ± 0.006b	0.160 ± 0.004b	14.124 ± 0.348b	2028 ± 14a	0.285 ± 0.016a	31.72 ± 1.06a	5.18 ± 0.00 bc
OS-4	0.538 ± 0.006b	0.165 ± 0.000ab	14.724 ± 0.072ab	2028 ± 24a	0.244 ± 0.003b	29.78 ± 0.59a	5.31 ± 0.11 b
RS	0.592 ± 0.004a	0.181 ± 0.004a	14.222 ± 0.210b	526 ± 2c	0.173 ± 0.003c	22.73 ± 0.08 b	6.32 ± 0.15 a

Values are means ± standard deviation. Values with different letters in the same column are significantly different at p < 0.05.

Table 3
Molar- and weight-based chain-length distribution of debranched amylopectin from starch samples.

Code	Weight-base distribution				Molar-base distribution			
	A(DP 6–12)	B_1(DP 13–24)	B_2(DP 25–36)	B_3(DP > 36)	A′(DP 6–12)	B'_1(DP 13–24)	B'_2(DP 25–36)	B'_3(DP > 36)
OS-1	16.81 ± 0.16b	55.66 ± 0.05a	16.39 ± 0.05a	11.13 ± 0.06bc	28.37 ± 0.30b	57.68 ± 0.20a	9.89 ± 0.06a	4.05 ± 0.03bc
OS-2	16.18 ± 1.25b	55.20 ± 1.24a	16.94 ± 0.23a	11.68 ± 0.22c	27.53 ± 2.72b	57.83 ± 2.37a	10.34 ± 0.35a	4.29 ± 0.00c
OS-3	16.83 ± 1.16b	54.59 ± 0.36a	16.69 ± 0.30a	11.88 ± 0.51c	28.33 ± 2.31b	57.14 ± 1.63a	10.17 ± 0.41a	4.37 ± 0.27c
OS-4	18.83 ± 2.79b	54.47 ± 2.69a	16.17 ± 0.47a	10.52 ± 0.37b	32.07 ± 5.52b	54.78 ± 4.84a	9.44 ± 0.65a	3.70 ± 0.03b
RS	23.30 ± 0.37a	46.06 ± 0.30b	13.42 ± 0.39b	17.23 ± 0.46a	41.26 ± 0.23a	44.63 ± 0.47b	7.92 ± 0.06b	6.19 ± 0.20a

Values are means ± standard deviation. Values in the same column with the same letters do not differ significantly ($P < 0.05$).

Table 4
Parameters obtained from fitting the number CLD of oat starches and rice starch.

Code	$\beta_{(i)}$	$\beta_{(ii)}$	$\beta_{(iii)}$	$\beta_{(iv)}$	$h_{(i)}$	$h_{(iii)}$
OS-1	0.0768 ± 0.0000b	0.0173 ± 0.0003b	0.0561 ± 0.0039a	0.0397 ± 0.0023c	0.8998 ± 0.0040b	0.0419 ± 0.0002a
OS-2	0.0745 ± 0.0010bc	0.0183 ± 0.0001b	0.0553 ± 0.0008ab	0.0558 ± 0.0022a	0.9022 ± 0.0039b	0.0430 ± 0.0019a
OS-3	0.0694 ± 0.0038c	0.0183 ± 0.0000b	0.0575 ± 0.0009a	0.0487 ± 0.0013b	0.8969 ± 0.0048b	0.0456 ± 0.0030a
OS-4	0.0775 ± 0.0033b	0.0140 ± 0.0008c	0.0506 ± 0.0004b	0.0487 ± 0.0017b	0.8946 ± 0.0058b	0.0363 ± 0.0022b
RS	0.0978 ± 0.0002a	0.0216 ± 0.0003a	0.0575 ± 0.0001a	0.0279 ± 0.0003d	0.9752 ± 0.0003a	0.0095 ± 0.0001c

Data are expressed as Means ± standard deviations. Different letters in the same column represent significant difference at $p < 0.05$.

from Table 3, there were less chains with DP 6–12 and DP > 37 and more chains with DP 13–24 and DP 25–36 in oat starches compared with rice starch.

3.4. Fitting the amylopectin number CLD with a mathematical model

The amylopectin number CLDs of all samples were well fitted with the mathematical model (Wang et al., 2015; Wu et al., 2013). All features were well reproduced in the fitted number CLDs for all samples as shown in Fig. S3, and the β values of the four enzyme sets obtained are given in Table 4. Significant differences were observed in the enzymatic activity between oat and rice starches, suggesting the differences in the enzyme action during starch biosynthesis of oat and rice. Small differences were also observed in the fitting parameters between oat starches, reflecting the differential effects of genetic variations on starch biosynthesis. From the model fitting, four β values ($\beta_{(i)}$, $\beta_{(ii)}$, $\beta_{(iii)}$ and $\beta_{(iv)}$), representing the relative activity of SBE to SS within each enzyme set (Li et al., 2016; Wang, Wambugu, et al., 2015), and another parameter h, reflecting the relative contribution of each enzyme set to the whole CLD, can be obtained. It is assumed in this model that four enzyme-sets are responsible for amylopectin biosynthesis. Chains with DP < 33 are predominately synthesized by enzyme-sets i and ii, while those with DP 33–80 are mainly by enzyme-sets iii and iv. Each enzyme-set includes one isoform of each of the SSs, SBEs and DBEs, and attributes to the features of the amylopectin CLD. Among the four enzyme sets, enzyme-sets i and iii play a more dominant role than enzyme-sets ii and iv, therefore, only h values for enzyme-sets i and iii, denoted $h_{(i)}$ and $h_{(iii)}$, were discussed in the present study.

As indicated from Table 4, rice starch had higher values of $\beta_{(i)}$ and $\beta_{(ii)}$, suggesting that enzyme sets i and ii have a higher SBE activity and/or a lower SS activity, consequently causing a higher proportion of branch points and/or more short amylopectin chains. Rice starch had a smaller value of $h_{(iii)}$, suggesting that the relative contribution of enzyme set ii is lower compared with oat starches. Apparent differences were observed in the β values among the four oat starches (Table 4), suggesting that the activity of SBEs in relative to that of SSs during amylopectin biosynthesis is different among the four oat starches. For example, the values of $\beta_{(ii)}$ and $h_{(iii)}$ of OS-4 were significantly lower than those of other starches, which may account for the different digestion properties and thermal properties of OS-4.

3.5. The relationship between digestion and molecular structure of starches

Native starch is digested slowly by enzymes, whereas cooking or processing increases its susceptibility to enzymatic breakdown (Wang & Copeland, 2013). In the present study, oat and rice starches were cooked at 100 °C for 30 min, which was assumed to completely disrupt the ordered structures of two starches (Wang, Sun, Wang, Wang, & Copeland, 2016). Hence, the differences in starch digestion profiles can only be attributed to the molecular structure of starches, namely size and chain length distribution of amylose and amylopectin molecules.

Oat starches showed a higher amylose content and larger amylose size than normal rice starch (Table 2 and Fig. 2), which may account for the slower digestion of OS-1 and OS-2es. However, this cannot explain the higher digestion rate of OS-3 and OS-4. Benmoussa, Moldenhauer, and Hamaker (2007) showed that rapidly digestible starch (RDS) in rice starch was negatively correlated with long (FrI, DP > 33) and intermediate/short (FrII, 13 < DP < 33) amylopectin linear chains, but positively correlated with very short linear chains (FrIII, DP < 13). Slowly digestible (SDS) starch was positively correlated with FrI and FrII, but negatively correlated with FrIII. Kong et al. (2015) also confirmed that the lower proportion of long branch chains (DP $\geqslant$ 37) and higher proportion of short A chains contributed to the higher RDS content in rice starch. As seen from Table 4, oat starch had a lower amount of the shortest A chains, which may also account for its lower digestion rate. However, the lower proportion of the longest B_3 chain may increase the digestion rate of oat starch. These structural features may lead to the small differences in digestion rate between oat starches (OS-3 and OS-4) and rice starch.

The lower values of $\beta_{(i)}$ and $\beta_{(ii)}$ of oat starches obtained from the biosynthesis model suggested that a lower SBE activity, and/or a higher SS activity led to a lower DB, consistent with the GPC results. A significant positive correlation between DB and d digestion rate has also been reported (Syahariza et al., 2013). The higher DB of amylopectin molecules may facilitate the access of enzymes to starch substrate, which accounts for the low digestion rates of OS-1 and OS-2.

4. Conclusions

In this study, the LOS plot was used to study the digestion property of oat starches, and GPC and HPAEC were used to characterize fine structure of amylose and amylopectin. Some oat starches (OS-1 and OS-2) had a slower digestion rate than the reference (rice) starch. Compared with rice starch, oat starches had higher amylose content, larger size of amylose lower amount of the shortest amylopectin chains, and lower DB values compared with rice starch, which may account for the slower digestion rate of oat starches. However, the lower proportion of the longest chains in oat starches may increase the digestion rate of oat starches. The complexity of theses structural features led to a small difference in digestion rate of OS-3, OS-4 and rice starch.

Acknowledgements

The authors would like to acknowledge the research funding from National Natural Science Foundation of China (31522043, 31301554).

Appendix A. Supplementary data

Supplementary data associated with this article can be found, in the online version, at http://dx.doi.org/10.1016/j.foodchem.2016.09.191.

References

Benmoussa, M., Moldenhauer, K. A., & Hamaker, B. R. (2007). Rice amylopectin fine structure variability affects starch digestion properties. *Journal of Agricultural and Food Chemistry, 55*(4), 1475–1479.

Butterworth, P. J., Warren, F. J., Grassby, T., Patel, H., & Ellis, P. R. (2012). Analysis of starch amylolysis using plots for first-order kinetics. *Carbohydrate Polymers, 87*(3), 2189–2197.

Chen, P., Wang, K., Kuang, Q., Zhou, S., Wang, D., & Liu, X. (2016). Understanding how the aggregation structure of starch affects its gastrointestinal digestion rate and extent. *International Journal of Biological Macromolecules, 87*, 28–33.

Chung, H.-J., Liu, Q., Lee, L., & Wei, D. (2011). Relationship between the structure, physicochemical properties and in vitro digestibility of rice starches with different amylose contents. *Food Hydrocolloids, 25*(5), 968–975.

Edwards, C. H., Warren, F. J., Milligan, P. J., Butterworth, P. J., & Ellis, P. R. (2014). A novel method for classifying starch digestion by modelling the amylolysis of plant foods using first-order enzyme kinetic principles. *Food & Function, 5*(11), 2751–2758.

Gudmundsson, M., & Eliasson, A.-C. (1989). Some physico-chemical properties of oat starches extracted from varieties with different oil content. *Acta Agriculturae Scandinavica, 39*(1), 101–111.

Hoover, R., Vasanthan, T., Senanayake, N. J., & Martin, A. M. (1994). The effects of defatting and heat-moisture treatment on the retrogradation of starch gels from wheat, oat, potato, and lentil. *Carbohydrate Research, 261*(1), 13–24.

Hu, X.-Z., Zheng, J.-M., Li, X.-P., Xu, C., & Zhao, Q. (2014). Chemical composition and sensory characteristics of oat flakes: A comparative study of naked oat flakes from China and hulled oat flakes from western countries. *Journal of Cereal Science, 60*(2), 297–301.

Kong, X., Bertoft, E., Bao, J., & Corke, H. (2008). Molecular structure of amylopectin from amaranth starch and its effect on physicochemical properties. *International Journal of Biological Macromolecules, 43*(4), 377–382.

Kong, X., Chen, Y., Zhu, P., Sui, Z., Corke, H., & Bao, J. (2015). Relationships among genetic, structural, and functional properties of rice starch. *Journal of Agriculture and Food Chemistry, 63*(27), 6241–6248.

Li, E., Hasjim, J., Dhital, S., Godwin, I. D., & Gilbert, R. G. (2011). Effect of a gibberellin-biosynthesis inhibitor treatment on the physicochemical properties of sorghum starch. *Journal of Cereal Science, 53*(3), 328–334.

Li, H., Prakash, S., Nicholson, T. M., Fitzgerald, M. A., & Gilbert, R. G. (2016). The importance of amylose and amylopectin fine structure for textural properties of cooked rice grains. *Food Chemistry, 196*, 702–711.

Patel, H., Day, R., Butterworth, P. J., & Ellis, P. R. (2014). A mechanistic approach to studies of the possible digestion of retrograded starch by α-amylase revealed using a log of slope (LOS) plot. *Carbohydrate Polymers, 113*, 182–188.

Poulsen, B., Ruiter, G., Visser, J., & Lønsmann Iversen, J. (2003). Determination of first order rate constants by natural logarithm of the slope plot exemplified by analysis of Aspergillus niger in batch culture. *Biotechnology Letters, 25*(7), 565–571.

Pu, J., & Hu, X. (2012). Nutraceutical properties and health benefits of oats. In *Cereals and pulses* (pp. 21–36). Wiley-Blackwell.

Syahariza, Z. A., Sar, S., Hasjim, J., Tizzotti, M. J., & Gilbert, R. G. (2013). The importance of amylose and amylopectin fine structures for starch digestibility in cooked rice grains. *Food Chemistry, 136*(2), 742–749.

Tosh, S. M., & Chu, Y. (2015). Systematic review of the effect of processing of whole-grain oat cereals on glycaemic response. *British Journal of Nutrition, 114*(8), 1256–1262.

Vilaplana, F., & Gilbert, R. G. (2010). Two-dimensional size/branch length distributions of a branched polymer. *Macromolecules, 43*(17), 7321–7329.

Wang, S., & Copeland, L. (2013). Molecular disassembly of starch granules during gelatinization and its effect on starch digestibility: A review. *Food & Function, 4*(11), 1564–1580.

Wang, K., Hasjim, J., Wu, A. C., Li, E., Henry, R. J., & Gilbert, R. G. (2015). Roles of GBSSI and SSIIa in determining amylose fine structure. *Carbohydrate Polymers, 127*, 264–274.

Wang, S., Li, C., Copeland, L., Niu, Q., & Wang, S. (2015). Starch retrogradation: A comprehensive review. *Comprehensive Reviews in Food Science and Food Safety, 14*(5), 568–585.

Wang, S., Sun, Y., Wang, J., Wang, S., & Copeland, L. (2016). Molecular disassembly of rice and lotus starches during thermal processing and its effect on starch digestibility. *Food & Function, 7*(2), 1188–1195.

Wang, K., Wambugu, P. W., Zhang, B., Wu, A. C., Henry, R. J., & Gilbert, R. G. (2015). The biosynthesis, structure and gelatinization properties of starches from wild and cultivated African rice species (Oryza barthii and Oryza glaberrima). *Carbohydrate Polymers, 129*, 92–100.

Wang, L. Z., & White, P. J. (1994). Structure and physicochemical properties of starches from oat with different lipid contents. *Cereal Chemistry, 71*, 443–450.

Wang, S., Zhang, X., Wang, S., & Copeland, L. (2016). Changes of multi-scale structure during mimicked DSC heating reveal the nature of starch gelatinization. *Scientific Reports, 2016*(6), 28271.

Wilfart, A. Y. J.-P., Simminsb, H., Nobleta, J., van Milgena, J., & Montagnec, L. (2008). Kinetics of enzymatic digestion of feeds as estimated by a stepwise in vitro method. *Animal Feed Science and Technology, 141*, 171–183.

Wu, A. C., & Gilbert, R. G. (2010). Molecular weight distributions of starch branches reveal genetic constraints on biosynthesis. *Biomacromolecules, 11*(12), 3539–3547.

Wu, A. C., Morell, M. K., & Gilbert, R. G. (2013). A parameterized model of amylopectin synthesis provides key insights into the synthesis of granular starch. *PLoS ONE, 8*(6), e65768.

Xu, D., Ren, G.-Y., Liu, L.-L., Zhu, W.-X., & Liu, Y.-H. (2014). The influences of drying process on crude protein content of naked oat cut herbage (Avena nuda L.). *Drying Technology, 32*(3), 321–327.

Zhou, M., Robards, K., & Glennie, M. (1998). Structure and pasting properties of oat starch. *Cereal Chemistry, 75*(3), 273–281.

Zou, W., Sissons, M., Gidley, M. J., Gilbert, R. G., & Warren, F. J. (2015). Combined techniques for characterising pasta structure reveals how the gluten network slows enzymic digestion rate. *Food Chemistry, 188*, 559–568.